ARO 18414.4-EG

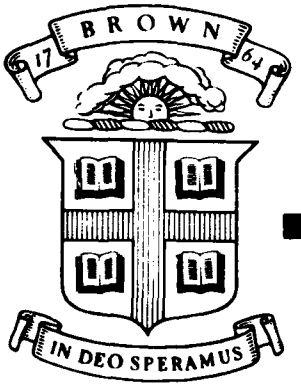

Division of Engineering
BROWN UNIVERSITY
PROVIDENCE, R. I.

INITIATION AND PROPAGATION OF SHEAR BANDS IN ANTIPLANE SHEAR DEFORMATION

F.H. Wu, M. Toulios and L.B. Freund

Army Research Office
Contract DAAG-29-81-K-0121
DAAG-0121/6 *Technical Report No. 6*

NSF Materials Research Laboratory
MRL E-151 *Brown University*

March 1984

Unclassified

SECURITY CLASSIFICATION OF THIS PAGE (When Data Entered)

REPORT DOCUMENTATION PAGE	READ INSTRUCTIONS BEFORE COMPLETING FORM
1. REPORT NUMBER: ARO 18414.4-EG	2. GOVT ACCESSION NO.: AD-A140 741
3. RECIPIENT'S CATALOG NUMBER	
4. TITLE (and Subtitle): Initiation and Propagation of Shear Bands in Antiplane Shear Deformation	5. TYPE OF REPORT & PERIOD COVERED: Technical Report
	6. PERFORMING ORG. REPORT NUMBER
7. AUTHOR(s): F. H. Wu, M. Toulios and L. B. Freund	8. CONTRACT OR GRANT NUMBER(s): DAAG29-81-K-0121
9. PERFORMING ORGANIZATION NAME AND ADDRESS: Brown Univ	10. PROGRAM ELEMENT, PROJECT, TASK AREA & WORK UNIT NUMBERS: N/A
11. CONTROLLING OFFICE NAME AND ADDRESS: U. S. Army Research Office, Post Office Box 12211, Research Triangle Park, NC 27709	12. REPORT DATE: Mar 84
	13. NUMBER OF PAGES: 39
14. MONITORING AGENCY NAME & ADDRESS(if different from Controlling Office)	15. SECURITY CLASS. (of this report): Unclassified
	15a. DECLASSIFICATION/DOWNGRADING SCHEDULE

16. DISTRIBUTION STATEMENT (of this Report)

Approved for public release; distribution unlimited.

17. DISTRIBUTION STATEMENT (of the abstract entered in Block 20, if different from Report)

18. SUPPLEMENTARY NOTES

The view, opinions, and/or findings contained in this report are those of the author(s) and should not be construed as an official Department of the Army position, policy, or decision, unless so designated by other documentation

19. KEY WORDS (Continue on reverse side if necessary and identify by block number)

Shear Bands
Shear Deformation
Strain Rate
Shear Stress
Strain Hardening

20. ABSTRACT (Continue on reverse side if necessary and identify by block number)

A large block of material is subjected to a constant average strain rate resulting in deformation in the antiplane shear mode. The material is assumed to be isotropic, incompressible and hyperelastic. To simulate the situation in which strain hardening of the material is overwhelmed by thermal softening, the shear stress as a function of shear strain has a local maximum. The block contains a material imperfection in the form of a small region in which the material is less stiff than the otherwise homogeneous block, and

DD FORM 1 JAN 73 1473 EDITION OF 1 NOV 65 IS OBSOLETE

UNCLASSIFIED

ARO 18414.4-EG

20. ABSTRACT CONTINUED:

in which the maximum possible stress is less than in the surrounding material. The transient deformation is analyzed numerically by means of the finite element method. It is found that a shear band initiates in the region of the material defect, and then propagates in a crack-like fashion into the rest of the body. A prediction of the speed of propagation of the edge of the band is made on the basis of a linearization of the governing field equations around a state corresponding to the strain level at which the local maximum in stress occurs.

INITIATION AND PROPAGATION OF SHEAR BANDS

IN ANTIPLANE SHEAR DEFORMATION

by

F. H. Wu, M. Toulios and L. B. Freund

Division of Engineering

Brown University

Providence, RI 02912 USA

INITIATION AND PROPAGATION OF SHEAR BANDS

IN ANTIPLANE SHEAR DEFORMATION

by

F. H. Wu, M. Toulios and L. B. Freund
Division of Engineering
Brown University
Providence, RI 02912 USA

Abstract

A large block of material is subjected to a constant average strain rate resulting in deformation in the antiplane shear mode. The material is assumed to be isotropic, incompressible and hyperelastic. To simulate the situation in which strain hardening of the material is overwhelmed by thermal softening, the shear stress as a function of shear strain has a local maximum. The block contains a material imperfection in the form of a small region in which the material is less stiff than the otherwise homogeneous block, and in which the maximum possible stress is less than in the surrounding material. The transient deformation is analyzed numerically by means of the finite element method. It is found that a shear band initiates in the region of the material defect, and then propagates in a crack-like fashion into the rest of the body. A prediction of the speed of propagation of the edge of the band is made on the basis of a linearization of the governing field equations around a state corresponding to the strain level at which the local maximum in stress occurs.

1. INTRODUCTION

The localization of deformation into shear bands is commonly observed during high strain rate inelastic deformation of metals and other materials. Such bands persist, once they are formed, and the subsequent deformation proceeds in a markedly nonuniform manner. Aside from their intrinsic scientific interest, such shear bands are of technical interest because they provide a deformation mode with an unacceptably low level of energy absorption for some applications and they are often precursory to fracture.

Experimental studies on shear bands have been carried out by Nadai (1931), Zener and Hollomon (1944), Rogers (1979) and more recently by Costin et al. (1979) and Moss (1980). Nadai has assembled a series of photographs of Luder's yielding in steel specimens, which demonstrated that the intense shear entails the crack-like propagation of bands in highly nonuniform conditions. The high strain rate and high temperature within the band, as reported by Rogers, Costin et al. and Moss, indicated that the deformation is nearly adiabatic and that a phase transformation may occur during deformation. The high temperature is thought to be due to the heat generated through dissipation of the mechanical work done to deform a material inelastically. If the deformation is very rapid, the heating process will be nearly adiabatic. Local heating tends to reduce the resistance of a material to further deformation which, in turn, leads to the generation of more heat, and so on. The material becomes unstable, in the sense of mechanical equilibrium, and a highly localized intense deformation develops, typically in the form of a shear band aligned with the direction of maximum shear stress.

Analytical studies were initially reported by Thomas (1961), Hill (1962) and Mandel (1966). In the latter two cases, shear bands were shown to correspond to stationary acceleration waves in elastic-plastic solids. More recently, Rudnicki and Rice (1975) and Rice (1976) addressed this problem for inelastic materials by seeking conditions for which the constitutive relations could allow a bifurcation from a homogeneous deformation state into a concentrated shear band mode. In a series of articles, Knowles and Sternberg (1978, and references therein) determined that the formation of surfaces with discontinuous displacement gradients in otherwise homogeneous nonlinear elastic solids is due to the loss of ellipticity in the equations of continuing equilibrium. These studies were concerned with the possible existence of

localizations, and the kinetics of formation was not addressed. An analysis of the evolution of a shear band under rising remote loads was presented by Abeyaratne and Triantafyllidis (1980). They introduced an imperfection in a large block of nonlinear elastic material (either heperelastic or hypoelastic), and they examined the differences between the uniform deformation field under rising load and the nonuniform field due to the imperfection by means of a regular perturbation analysis. They concluded that the shear localization behavior may be exhibited if the incremental equilibrium equations loose ellipticity. Moreover, they found that the effect of the imperfection on the deformation field was very small until the remote uniform stretch reached values which were very close to the critical value at which the equations for uniform tensile deformation loose ellipticity.

An alternative approach to the study of the criteria for the onset of shear localization in one dimensional models has been considered by some authors, including Recht (1964), Argon (1973), Culver (1973) and Staker (1981). They have proposed instability criteria (i.e., criteria for the formation of a shear band) based on the attainment of a local maximum in the dependence of shear stress on shear strain during a homogeneous deformation. In a departure from the notion of a criterion based on a stress maximum, Clifton (1980), Bai (1980), and Burns and Trucano (1982) examined the growth of infinitesimal periodic nonuniformities in an otherwise uniform simple shearing deformation in a material exhibiting strain hardening, thermal softening and strain rate sensitivity. Clifton and Bai assumed that the basic material parameters occurring in the problem, such as the strain hardening and thermal softening parameters, are time independent. They found that the magnitude of the nonuniformities may grow or decay in time, depending on the material parameters, the average strain rate, and the fixed spatial wavelength of the initial periodic nonuniformity. Burns and Trucano extended the study and allowed the material properties to be time dependent. They found that the stability prediction for time-dependent material properties is somewhat different from that based on time independent properties in the adiabatic limit.

The growth of a shear band and the dependence of its width on material properties, such as strain hardening and thermal conductivity characteristics, has been carried out by Wu and Freund (1984). They considered an imperfection-free half-space subjected to a time dependent but spatially uniform tangential loading. The half-space material exhibited strain hardening, thermal softening and strain rate

sensitivity. They applied the wave trapping idea (cf., Erlich et al. (1980)) in the numerical simulation of plastic shear wave propagation under adiabatic conditions, as well as with heat conduction included. It was found that thermal conduction made the shear band slightly narrower. They also considered both linear dependence and lagarithmic dependence of the flow stress on the strain rate, and found that the band thickness varied with rate of loading differently for these two types of rate sensitivity.

The mechanism by which shear bands evolve under high rates of loading is not clear, but it appears that their formation is quite abrupt. One possibility is that they initiate due to strain concentrations at material or geometrical defects, and that they propagate in a crack-like fashion to become the bands observed in laboratory specimens. In this discussion, the phenomenon is studied from this point of view. The two dimensional antiplane shear deformation of a large block of material is considered. As a first attempt at examining the shear band propagation process, the material is assumed to be hyperelastic and incompressible at each point. Furthermore, to simulate the phenomenon of thermal softening due to adiabatic heating, a material model is selected which shows a local maximum in the dependence of shear stress on shear strain. The block contains a small region in which the stiffness is less than in the remainder of the otherwise homogeneous material, and this small region is called the defect. Initially, the block is supposed to have no strain and a spatially uniform strain rate. At points remote from the defect (compared to the size of the defect), loads are applied to produce a constant average strain rate for later times. While the field equations do not appear to admit a complete analytical solution, two simple analyses are first carried out to shed some light on the nature of the transient fields. If the field equations are written in a form sutiable for analysis of plane wave propagation, then an equation for the speeds of propagation of acceleration waves may be obtained. The direction of the growing shear band is determined by examining the inclination of an acceleration wave which becomes stationary as a result of the local strain field attaining the critical value (corresponding to the local maximum in stress in the constitutive relation). In addition, the field equations may be linearized about the ongoing uniform background strain. The resulting wave equation, which is linear but with time dependent coefficients, contains the influence of the defect as a forcing term. The wave speed resulting from this wave equation provides an estimate of the speed of propagation of the edge of the shear band which grows from the defect. Finally, a complete numerical solution of the problem is obtained by means of the finite element

discretization of the body and by the use of a finite difference method to intergrate the differential equations for the evolution of the nodal variables in the finite elements. It is found that the strain in the block remains more or less uniform up until the time at which the condition for instability is met in the defect. Strain is rapidly concentrated at the edge of the defect, and a shear band grows at very high speed from the defect out into the remainder of the block. It is important to note that this happens for average strain levels which are substantially below the critical strain level for the material outside of the defect. The speed of propagation of the edge of the band compares very well with the estimate of speed obtained from the linearized analysis.

2. MATERIAL MODEL

In the linearized theory of elasticity, nontrivial equilibrium fields of antiplane shear are possible in the absence of body forces for any homogeneous, isotropic material. However, according to the discussion of Adkins (1954), this cannot be expected for the exact theory of antiplane shear deformation in finite elasticity. In contrast, it shows that there must be some restriction on the strain energy function of the material in order to allow for nontrivial two dimensional out-of-plane displacement fields. Knowles (1976) has provided the necessary and sufficient condition for a homogeneous, isotropic, incompressible material to admit nontrivial states of antiplane shear, and the material models used here comply with this conditon.

The second restriction on the material considered here is that there must exist a critical strain beyond which the field equations governing equilibrium fields loose ellipticity for homogeneous deformations. Compliance with this restriction will allow for the possibility of initiating shear bands and, for antiplane shear, the existence of a local maximum in the dependence of shear stress on shear strain is necessary and sufficient.

Following Knowles (1977), we consider the material with the strain energy function $W(I_1)$ defined by

$$W(I_1) = \frac{\mu_o}{2b}\left(\left[1 + \frac{b}{n}(I_1 - 3)\right]^n - 1\right), \qquad I_1 \geq 3 \tag{2.1}$$

where I_1 is the first invariant of the left Cauchy-Green deformation tensor. If $u(x_1, x_2)$ is the antiplane displacement parallel to the x_3 direction, then

$$I_1 = 3 + u_{,\alpha}\, u_{,\alpha} \tag{2.2}$$

in which the Greek indices take the values 1,2 and repeated indices imply summation over this range. An index following a comma denotes partial differentiation with respect to the corresponding coordinate. The material description (2.1) involves three material paramaters, namely, the shear modulus for infinitesimal deformations μ_o, the hardening parameter n, and the positive dimensionless parameter b. If $n = 1$ then the material is linearly elastic. If n is in the range $0.5 < n < 1$ then the stress increases indefinitely

with increasing strain. And if $0 < n < 0.5$ then the stress has a local maximum with increasing strain.

For the ideal material defined by (2.1), the Cauchy stress-strain relation for antiplane shear deformation is

$$\begin{aligned} \tau_{3\alpha} &= \tau_{\alpha 3} = 2W'(I_1)\, u_{,\alpha} \\ \tau_{33} &= 2W'(I_1)\, u_{,\alpha}\, u_{,\alpha} - d_0(x_3 + u) - d_1 \\ \tau_{\alpha\beta} &= 0 \end{aligned} \tag{2.3}$$

where the prime denotes differentiation with respect to I_1, and d_0 and d_1 are constants to be determined by the boundary conditions. Introducing the quantities

$$\tau = \sqrt{\tau_{31}^2 + \tau_{32}^2}\,, \qquad k = u_{,\alpha}\, u_{,\alpha} \tag{2.4}$$

as measures of the shear stress magnitude and the shear strain magnitude, respectively, in the body, the constitutive relation between τ and k for the material being considered here is

$$\tau = 2kW'(3 + k^2) = \mu_o k\left[1 + \frac{b}{n}k^2\right]^{n-1} \tag{2.5}$$

The relationship between τ and k is shown for several values of n and b in Fig. 1. As can be seen from the figure, τ is a monotically increasing function of k for $n > 0.5$. On the other hand, there exists a local maximum in stress for $0 < n < 0.5$. The value of k at which the maximum in stress occurs is $k = \sqrt{n/b(1-2n)}$.

3. FORMULATION

A rectangular cartesian coordinate system is introduced so that the x_1, x_2-plane is the plane of deformation, and all field quantities are independent of x_3. In addition, there exists a region around the origin of coordinates in which the material offers less resistance to deformation than the material in the remainder of the body. A schematic of the configuration is shown in Fig. 2. Initially, the displacement is zero and the particle velocity varies linearly with x_2 according to

$$v(0, x_1, x_2) = ax_2 \tag{3.1}$$

Thus, a represents the uniform average strain rate. For later times, the velocity field at points remote from the defect (compared to the size of the defect) is forced to have the form (3.1). For points in the vicinity of the defect, however, the velocity field is allowed to evolve according to the field equations. If the body were homogeneous, then the velocity field (3.1) would provide a solution to the field equations for all times. Because of the presence of the defect in the present case, strains will become concentrated near the defect and, under suitable conditions, a shear band will be initiated.

The only nontrivial momentum equation for antiplane shear is

$$\frac{\partial \tau_{13}}{\partial x_1} + \frac{\partial \tau_{23}}{\partial x_2} = \rho \frac{\partial^2 u}{\partial t^2} \tag{3.2}$$

in which t denotes time. The constant d_0 in (2.3) is equal to zero because the end faces of the body, at $x_3 = \pm L$, say, are free of normal traction. Substituting from (2.3) for the stress in terms of the displacement gradient into (3.2) yields

$$\frac{\partial}{\partial x_\alpha}\left[2W'(I_1)\frac{\partial u}{\partial x_\alpha}\right] - \rho \frac{\partial^2 u}{\partial t^2} = 0 \tag{3.3}$$

which is a second order quasilinear partial differential equation for the dispalcement as a function of x_1, x_2, t.

One of several ways of introducing the concept of characteristic surfaces (cf., Courant and Hilbert, 1962) is as a surface $\psi(x_1, x_2, t) = 0$ for which a well-posed Cauchy problem cannot be solved in general.

When this is the case, the normal derivative $\partial^2 u/\partial\psi^2$ will be indeterminate on this surface. Consequently, certain fields may be discontinuous across the surface without violating the conditions imposed through the field equations.

If new independent variables are introduced so that the ψ coordinate is normal to a prospective characteristic curve in the $t = constant$ plane, and the other "spatial" coordinate is along the curve, then the equation (3.3) takes the form

$$[2W'\psi_{,\alpha}\,\psi_{,\alpha} + 4W''u_{,\alpha}\,u_{,\beta}\,\psi_{,\alpha}\,\psi_{,\beta} - \rho\psi_{,t}^2]\frac{\partial^2 u}{\partial\psi^2} + R = 0 \tag{3.4}$$

The quantity R represents the terms which can be determined from the Cauchy data. From its definition, the curve $\psi = 0$ is a characteristic curve if the coefficient of $\partial^2 u/\partial\psi^2$ in (3.4) is equal to zero. This condition may be written in the form

$$\begin{aligned}(W' + 2W''u_{,1}^2)\left(\frac{\partial\psi}{\partial x_1}\right)^2 + (W' + 2W''u_{,2}^2)\left(\frac{\partial\psi}{\partial x_2}\right)^2 \\ +4W''u_{,1}\,u_{,2}\,\frac{\partial\psi}{\partial x_1}\frac{\partial\psi}{\partial x_2} - \rho\left(\frac{\partial\psi}{\partial t}\right)^2 = 0\end{aligned} \tag{3.5}$$

If the direction n_α and the speed V are now introduced as

$$n_\alpha = \frac{\partial\psi/\partial x_\alpha}{\psi_{,\beta}\,\psi_{,\beta}} \tag{3.6}$$

$$V = -\frac{\partial\psi/\partial t}{\sqrt{\psi_{,\beta}\,\psi_{,\beta}}} \tag{3.7}$$

then n_α is obviously the unit normal to the spatial characteristic curve $\psi = 0$ and V is the corresponding speed of propagation. The curve $\psi = 0$ may also be interpreted as an acceleration wave (cf., Truesdell, 1961). Furthermore, due to the nature of antiplane deformations, the speed of propagation of this wave does not depend on the particle velocity. The substitution of (3.6) and (3.7) into (3.5) gives the characteristic condition

$$(W' + 2W''u_{,1}^2)n_1^2 + (W' + 2W''u_{,2}^2)n_2^2 + 4W''u_{,1}\,u_{,2}\,n_1 n_2 = \rho V^2 \tag{3.8}$$

The condition for the formation of a shear band could be viewed as being equivalent to the condition for the acceleration wave to become stationary, that is, for its speed to become zero. Therefore, it is possible to find the direction of the stationary wave front, or the plane on which a band forms, by setting $V = 0$ in the characteristic condition (3.8). Hence,

$$\frac{n_1}{n_2} = -\frac{2W'' u_{,1}\, u_{,2} \pm \sqrt{(-W')(W' + 2W'' u_{,\alpha}\, u_{,\alpha})}}{W' + 2W'' u_{,1}^2} \tag{3.9}$$

For the particular form of the strain energy function being used here, (3.9) becomes

$$\frac{n_1}{n_2} = \frac{2(1-n)\frac{b}{n} u_{,1}\, u_{,2} \pm \sqrt{-(1 + \frac{b}{n} u_{,\alpha}\, u_{,\alpha})(1 + (2n-1)\frac{b}{n} u_{,\beta}\, u_{,\beta})}}{(2n-1)\frac{b}{n} u_{,1}^2 + 1 + \frac{b}{n} u_{,2}^2} \tag{3.10}$$

Inspection of (3.10) and comparison with the stress-strain relation (2.5) reveals that real values of the ratio n_1/n_2 are first possible for values of strain corresponding to the maximum in the $\tau - k$ relationship, that is, for $u_{,\alpha}\, u_{,\alpha} = n/[b(1-2n)]$. This implies that the two dimensional problem of antiplane shear has basic features in common with the wave-trapping concept mentioned in the Introduction and invoked by Wu and Freund (1984). Moreover, it can be demonstrated that the equation of equilibrium suffers a loss of ellipticity when this same maximum point in the $\tau - k$ relationship is reached (Zee and Sternberg, 1983).

In addition, it is evident that the value of the ratio n_1/n_2 in (3.10) will depend on the boundary conditions in any actual deformation field. For the problem at hand, the background deformation field has a large strain component in the x_2 direction and no strain in the x_1 direction. Consequently, it can be anticitpated that $n_1/n_2 = 0$ and the shear band will grow in the x_1 direction. This expectation is borne out by the results of the finite element calculation.

One special case of interest is when the exponent n is equal to $1/2$. As can be seen from (3.10), the ratio n_1/n_2 is then

$$\frac{n_1}{n_2} = \frac{2b u_{,1}\, u_{,2} \pm \sqrt{-1 - 2b\, u_{,\alpha}\, u_{,\alpha}}}{1 + 2b\, u_{,2}^2} \tag{3.11}$$

which is always imaginary and, therefore, no stationary waves can exist. Effectively, the same conclusion can be reached by means of the numerical calculation, and this is further discussed in section 5.

4. FINITE ELEMENT FORMULATION

The field equations are satisfied in the weak, or variational, sense of finite elements. The lengths h_1 and h_2 are large compared to the size of the defect. The boundary conditions are chosen so that the far-field particle velocity (3.1) is imposed on $x_1 = h_1$ and $x_2 = h_2$, the symmetry condition of zero displacement is enforced on $x_2 = 0$ and the symmetry condition of zero normal derivative of displacement is enforced on $x_1 = 0$.

The stress-strain relation of the material and the equation of momentum balance are

$$\begin{aligned} \tau_\beta &= \mu\left[1 + \frac{b}{n} u_{,\alpha}\, u_{,\alpha}\right]^{n-1} u_{,\beta} \\ \tau_{\beta,\beta} &= \rho v_{,t} \end{aligned} \tag{4.1}$$

subject to the boundary conditions

$$\begin{aligned} v(t, x_1, 0) &= 0 \\ v(t, x_1, h_2) &= a h_2 \\ v_{,1}(t, 0, x_2) &= 0 \\ v(t, h_1, x_2) &= 0 \end{aligned} \tag{4.2}$$

The initial condition is given by (3.1). In the foregoing equations, u is the particle displacement and v is the particle velocity, respectively, in the x_3 direction. Also, in these equations and in the analysis that follows, $\tau_{\alpha 3}$ is replaced by τ_α The material constants b, n, and μ are the same as those introduced in the preceding section, except that now μ varies with position x_1, x_2 to simulate the presence of the material defect. The particular form

$$\mu = \mu_0[1 + \epsilon F(x_1, x_2)] \tag{4.3}$$

is assumed for this variation, where μ_0 is the constant infinitesimal shear modulus of the material outside of the defect and the function F, which vanishes outside of the defect, describes the material variation within the defect. The shape function is chosen to have continuous first derivatives.

It is convenient to introduce nondimensional coordinates and field quantities as follows:

$$\xi_1 = \frac{x_1}{h_1} \qquad \xi_2 = \frac{x_2}{h_2} \qquad \eta = \frac{c_o}{h_2}t$$
$$w = \frac{u}{h_2\gamma_o} \qquad \phi = \frac{\partial w}{\partial \eta} = \frac{v}{c_o\gamma_o} \tag{4.4}$$

where c_o is the speed of infinitesimal elastic waves,

$$c_o = \sqrt{\mu_o/\rho} \tag{4.5}$$

and ρ is material mass density. For $n < 0.5$, γ_o is the critical strain at which the shear stress (2.5) reaches its maximum value. In terms of the material parameters, γ_o is given by

$$\gamma_o = \left[\frac{n}{b(1-2n)}\right]^{1/2} \tag{4.6}$$

If stress is elimated from (4.1) then the field equations may be written in the form of a first order system of partial differential equations in terms of the nondimensional variables as follows,

$$\rho\frac{c_o^2\gamma_o}{h_2}\phi_{,\gamma} = \left[\mu\left[1 + \frac{b}{n}(h_2\gamma_o)^2 w_{,\alpha}\, h_{\underline{\alpha}}^{-2}\right]^{n-1} h_2\gamma_o w_{,\beta}\, h_{\underline{\beta}}^{-1}\right]_{,\beta}\, h_{\underline{\beta}}^{-1} \tag{4.7}$$

where a bar under a subscript is used to indicate that it is to be viewed as an exception to the summation convention, and subscripts following a comma denote differentiation with respect to the corresponding nondimensional coordinate. The boundary conditions are

$$\begin{aligned} \phi(\eta, \xi_1, 0) &= 0 \\ \phi(\eta, \xi_1, 1) &= \frac{ah_2}{c_o\gamma_o} \\ \phi_{,1}(\eta, 0, \xi_2) &= 0 \\ \phi(\eta, 1, \xi_2) &= 0 \end{aligned} \tag{4.8}$$

in terms of the nondimensional variables, and the initial conditions are

$$\begin{aligned} \phi(0, \xi_1, \xi_2) &= \frac{ah_2}{c_o\gamma_o}\xi_2 \\ w(0, \xi_1, \xi_2) &= 0 \end{aligned} \tag{4.9}$$

In order to obtain a numerical solution of the equations above, Galerkin's principle is applied to satisfy the equations in a weak sense. Both sides of the first equation in (4.7) are multiplied by a function,

say ϕ^*, which is arbitrary except that it must have the same smoothness properties and must satisfy the same kinematic conditions as ϕ, and then are integrated over the rectangular region in Fig. 2. This region is divided into a 40 by 40 array of like rectangles, each of which is composed of two constant strain triangles. Application of the divergence theorem leads to

$$\int \phi_{,\eta}\, \phi^*\, dA = -\int (1+\epsilon f)\left[1+\frac{b}{n}(h_2\gamma_o)^2 w_{,\alpha}^2\, h_\alpha^{-2}\right]^{n-1} h_2^2 h_\beta^{-2} w_{,\beta}\, \phi_{,\beta}^*\, dA \tag{4.10}$$

where $f(\xi_1, \xi_2)$ is the imperfection shape function viewed as a function of the nondimensional spatial coordinates. The rectangular region is then divided into triangular finite elements as indicated in Fig. 2, and both the displacement field and velocity field are expressed approximately in terms of their nodal values in the usual way, that is,

$$\begin{aligned} \phi &= \phi_i \delta_i \\ w &= w_i \delta_i \end{aligned} \tag{4.11}$$

where the interpolation functions δ_i varies linearly within each element, and it has the value one at the $i-th$ node and the value zero at all other nodes. Summation over all nodes in the finite element array is assumed in (4.11). Likewise,

$$\phi^* = \phi_i^* \delta_i \tag{4.12}$$

In view of the fact that ϕ_i^* is arbitrary, the variational statement of the governing equations (4.10) may be reduced to a system of ordinary differential equations in η for the nodal values of the field quantities,

$$\begin{aligned} M_{(ij)}\phi_{j,\eta} &= R_i(w_j;\epsilon) \\ w_{i,\eta} &= \phi_i \end{aligned} \tag{4.13}$$

where $M_{(ij)}$ is the constant (lumped) mass matrix. The system of differential equations (4.13) is solved numerically by means of the forward finite difference scheme as discussed by Zienkiewicz (1977). Numerical experiments were performed to establish limits on the time-step range required for stability of the scheme and to test the accuracy of the scheme for calculations which involve many time steps.

In the calculations, a form for the imperfection shape function is required. In all calculations, it was

assumed that

$$f(\xi_1, \xi_2) = \begin{cases} (\xi_1^2 - d^2)^2(\xi_2^2 - d^2)^2/d^8, & \text{if } \xi_1 \leq d \text{ and } \xi_2 \leq d \\ 0, & \text{if } \xi_1 > d \text{ or } \xi_2 > d \end{cases} \tag{4.14}$$

The value $d = 0.1$ was used in generating all of the results being presented in this report. This implies that the size of the imperfection is approximately one-tenth of the size of the region over which the governing equations are solved numerically. Because the shape function (4.14) has a continuous derivative, however, the material weakness is actually confined to a somewhat smaller region. Three different values for the strength of the imperfection ϵ were selected, namely, $\epsilon = -0.25, -0.5$, and -0.75, for calculations done with the particular value of hardening (or softening) parameter $n = 0.4$. This corresponds to the relative rate of adiabatic softening observed in high strength steels (cf. Culver(1973)).It is found that the speed of propagation of the band is not sensitive to the strength of the defect, but the strength ϵ does influence the magnitude of the strain within the region of deformation localization. The difference is due mainly to the fact that a shear band initiates at a smaller level of background strain for a stronger imperfection (larger magnitude of ϵ), so that more strain has accumulated at any given time. The results in the following sections are based almost entirely on calculations done with $\epsilon = -0.5$.

5. RESULTS

In order to get a better understanding of the influence of the parameter n on the propagation speed of a shear band, calculations were performed for several values of n, namely, $n = 0.4$, 0.45 and 0.5. The loading rate parameter $ah_2/c_o\gamma_o$ was assumed to have the value 0.2. Physical parameters which would result in this value are, for example, an elastic wave speed of $3000m\,s^{-1}$, an imposed strain rate of $3000s^{-1}$, a transverse dimension of the block of $0.2cm$, and a critical strain level of 0.01.

First, the distribution of particle velocity ϕ and shear strain γ_{23} along the line $\xi_1 = 2d$ are shown for the case $n = 0.4$. The nodal values of the velocity ϕ are shown for different times in Fig. 3, and the variation of the strain component γ_{23} (which is uniform within an element) is shown in Fig. 4. The stages in the nucleation of a band are evident in Fig. 3. Initially, the particle velocity is nearly linear across the section. As the deformation advances and the differences in material stiffness becomes evident, material particles accelerate for points near the defect (due to reduced resisting stress). The diminishing resistance of the material near the defect to deformation causes an unloading wave to propagate into the block. The strain distribution shown develops accordingly, as shown in Fig. 4. The uniform strain distribution gives way to a distribution which is highly localized in the region of the defect and which shows relaxation at points away from the defect. The general features of the distribution shown in Fig. 4 are similar to those observed in the one-dimensional analysis considered by Wu and Freund (1984).

In order to investigate the propagation of the shear band in the x_1 direction, the distribution of velocity ϕ in the ξ_1 direction for $\xi_2 = d/4$ is shown in Fig. 5 for several values of the time parameter η. In addition, the distribution of strain γ_{23} in the ξ_1 direction for the first row of elements ($0 < \xi_2 < d/4$) is shown in Fig. 6 for several values of the time parameter η. From Fig. 5, it is evident that the particle velocity increases rapidly at a material point as the edge of the band approaches, and that the velocity decreases equally rapidly after the edge passes by the observation point. The variation of particle velocity shown in Fig. 5 is reminiscent of the correspoinding result for a particle near the fracture plane of a growing crack as the crack tip passes by. The rapid variations in particle velocity suggest that material inertia may play a significant role in the shear band growth process.

Because they were unable to observe partially developed shear bands in their experiments, Costin

et al. (1977) concluded that the speed of propagation of the edge of the bands must be very fast, even on the time scale of a dynamic experiment conducted with the Kolsky-bar apparatus. To obtain an estimate of the speed of propagation of the edge of the bands for the present model, the data in Fig. 6 were used. It was noted that, after the band was well-developed, fixed levels of strain propagated at almost constant speed. For example, if attention is focused on the strain level 0.02, it is found that the speed of propagation is approximately $0.57c_o$ for $n = 0.4$. If the same calculation is done for $n = 0.45$, then the speed of propagation is found to be about $0.48c_o$. Recall that c_0 is the speed of infinitesimal elastic waves.

In the Appendix, a simple analysis is described in which the governing equations for the problem at hand are linearized around the ongoing background strain. It is found that the displacement field is governed by a linear wave equation with time dependent coefficients; see (A.3). If the speed of propagation of disturbances in the x_1 direction is estimated from the equation at that time at which the coefficient of the term $u_{,22}$ vanishes, then the following result is obtained,

$$c = c_o\left(\frac{2-2n}{1-2n}\right)^{(n-1)/2} \tag{5.1}$$

The propagation speed obtained from this simple approach was quite close to the speed observed from the computed fields for all cases tested, always within 10%. For example, for $n = 0.4$, the estimate from (5.1) is $0.584c_o$; for $n = 0.45$, the estimate is $0.517c_o$.

In order to get a view of the complete fields at a fixed time, results in the form of Figs. 7 and 8 were generated. Fig. 7 is intended to show the complete particle velocity distribution as a surface over the ξ_1, ξ_2 plane at a fixed instant of time. The particle velocity at a point is the elevation of the surface over that point. The concentration of velocity around the edge of the band is evident from the figure. Fig. 8 shows the distribution of the strain component γ_{23} for the same time. The strain is clearly quite uniform over the whole block, except for points on the shear band where the strain levels are many times higher than the ongoing background strain.

To illustrate the complexity of the stress history experienced by a material particle due to the passage of a shear band edge, the trajectory of the stress point in stress space is shown in Fig. 9 for the

element adjacent to the symmetry plane $\xi_2 = 0$ at $\xi_1 = 2d$. In the early stage of the process, the stress component τ_1 is essentially zero and the component τ_2 develops within the uniform ongoing strain field. As the band edge approaches, the stress state deviates from being proportional but, some time after the edge of the band has passed, the state again becomes one-dimensional. Actually, the stress history in the second row of elements from the symmetry line $\xi_2 = 0$ for $\xi_1 = 2d$ shows a greater divergence, as shown in Fig. 10. This stress history resembles the stress history experienced by a material particle near the fracture plane due to passage of the edge of a crack.

A full set of results was also computed for $n = 0.45$, and the general features described for $n = 0.4$ above were again obtained. The calculations were repeated for $n = 0.5$ which is the value of the hardening parameter for which the stress- strain relation has a horizontal asymptote for very large values of strain but the stress does not have a local maximum at any finite strain level. In this case, no stationary acceleration wave can exist so that, based on the approach taken in section 3, a shear band is not anticipated. The strain distributions analogous to Figs. 4 and 6 for $n = 0.5$ are shown in Figs. 11 and 12, respectively. Obviously, the material defect acts as a strain concentrator and the strain intensifies at points near the defect. However, a shear band which propagates away from the defect is not observed in this case. Instead, a diffuse nonlinear zone (like a crack tip plastic zone in a hardening material) gradually expands away from the defect.

6. DISCUSSION

A nonlinear elastic material with an imperfection under finite antiplane derformation has been modeled to illustrate the process of formation and propagation of a band of intense shear deformation. Several observations of a general nature can be made concerning this analysis. For example, the effect of the imperfection on the ongoing background deformation field is very small until the strain within the defect region reaches a critical value for instability. The resulting load transfer to material adjacent to the defect causes a strain concentration which rapidly forms into a narrow band or layer which subsequently propagates in a crack-like fashion through the homogeneous material outside the defect region. Because the material has no viscosity, the thickness of the layer would be vanishingly small if the field equations were satisfied pointwise. In the present case, with the resolution of the analysis set by the finite element mesh, the thickness of the band or layer is always found to be one mesh spacing.

Numerical experiments were conducted in order to investigate the influence of the strength of the initial imperfection on the evolution of the shear layer. Of course, it was found that if the critical strain for instability within the defect were increased toward the critical strain for instability in the otherwise homogeneous block of material, then the shear band was nucleated at a higher level of background strain. However, it was found that the speed of propagation of the edge of the shear band, once formed, was not sensitive to the level of background strain at which the band formed. That is, once the band was formed, its growth seemed to be sustained by the natural strain concentration at the edge of the band, no matter what the level of background strain. If this feature carries over to the description of the process for more realistic material models, it would cast some doubt on the applicability of one dimensional shear models in the study of band formation in materials. The one dimensional models require that some sort of instability criterion be met globally in order for a band to form, whereas the two dimensional band growth model incorporates a natural strain concentrator at the edge of the band so that an instability criterion must be met only locally for the band to evolve.

Finally, the limitation of the present analysis to elastic (that is, inviscid and path-independent) material response is a serious deficiency in considering application of the results in the interpretation of experimental data on adiabatic shear band formation in real materials. It is anticipated that the inclusion

of strain rate sensitivity in the description of material response would inhibit the formation of the band at the defect, whereas the inclusion of plasticity effects would provide stabilization of the band growth process, analogous to its influence in plastic crack growth in fracture mechanics. The investigation is continuing, with primary attention being devoted to the incorporation of more realistic material models in the analysis.

ACKNOWLEDGEMENTS

The research support of the Army Research Office - Durham and of the NSF Materials Research Laboratory at Brown University is gratefully acknowledged.

The computations were performed on the VAX11/780 Engineering Computer Facility at Brown University. This Facility was made possible by grants from the National Science Foundation (Solid Mechanics Program), the General Electric Foundation, and the Digital Equipment Corporation.

REFERENCES

Abeyaratne, R. and Triantafyllidis, N. , "The Emergence of Shear Bands in Plane Strain, " *Int. J. Solids Structures*, Vol. 17, No. 12, p. 1113, 1981.

Adkins, J. E. , "Some Generalizations of The Shear Problem for Isotropic Incompressible Materials, " *Proc. Cambridge Philos. Soc. ,* Vol. 50, p. 334, 1954.

Argon, A. S. , "Stability of Plastic Deformation," Chap. 7 in *The Inhomogenity of Plastic Deformation*, ASM, Metals Park, OH, p. 161, 1973.

Bai, Y. L. , "A Criterion for Thermo-Plastic Shear Instability, " Chap. 17, in *Shock Waves and High-Strain-Rate Phenomena in Metals*, Meyers, M. A. , Murr, L. E. (eds.), Plenum Press, New York and London, p. 277, 1980.

Burns, T. J. and Trucano, T. G. , "Instability in Simple Shear Deformations of Strain-Softening Materials, " *Mechanics of Materials*, Vol. 1, No. 4, p. 313, 1982.

Clifton, R. J. , "Adiabatic Shear Banding, " Chap. 8, in *Materials Response to Ultra High Loading Rates*, National Materials Advisory Board Committee, Rep. No. NMAB-356, 1980.

Costin, L. S. , Chrisman, E. E. , Hawley, R. H. and Duffy, J. , "On The Localization of Plastic Flow in Mild Steel Tubes under Dynamic Torsional Loading, " Brown University Technical Report, NSF18532/7, 1979.

Courant, R. and Hilbert, D. , *Methods of Mathematical Physics*, Vol. II, Interscience, N. Y. , 1962.

Culver, R. S. , "Thermal Instability Strain in Dynamic Plastic Deformation, " in *Metallurgical Effects at High Strain Rates*, Rhode, R. W. , Butcher, B. M. , Holland, J. R. and Karnes, C. H. (eds.), Plenum Press, NY, p. 519, 1973.

Erlich, D. C. , Curran, D. R. and Seaman, L. , "Further Development of A Computational Shear Band Model, " Army Materials and Mechanics Research Center, Rep. No. AMMRC TR 80-3, March 1980.

Hayes, M. and Rivlin, R. S. , "Propagation of A Plane Wave in An Isotropic Elastic Material Subjected to Pure Homogeneous Deformation, " *Arch. Rational Mech. Anal.* , Vol. 8, p. 15, 1961.

Hill, R. , "Acceleration Waves in Solids, " *J. Mech. Phys. Solids*, Vol. 10, p. 1, 1962.

Knowles, J. K. , "On Finite Anti-Plane Shear For Incompressible Elastic Materials, " *J. Austrial. Math. Soc.* , Vol. 19 (series B), p. 400, 1976.

Knowles, J. K. , "The Finite Anti-Plane Shear Field Near The Tip of A Crack for A Class of Incompressible Elastic Solids, " *Int. J. of Fracture*, Vol. 13, No. 5, 1977.

Knowles, J. K. and Sternberg, E. , "On The Failure of Ellipticity and The Emergence of Discontinuous Deformation Gradients in Plane Finite Elastostatics, " *J. Elasticity*, Vol. 8, p. 329, 1978.

Mandel, J. , "Conditions de Stability et Postulate de Drucker, " *Rheology and Soil Mechanics*, Kravtchenko, J. and Sirlieys, P. M. (eds.), Springer-Verlag, Berlin, p. 58, 1966.

Moss, G. L. , "Shear Strains, Strain Rates and Temperature Changes in Adiabatic Shear Bands," Chap. 19, in *Shock Waves and High-Strain-Rates Phenomenon in Metals*, Meyers, M. A. , Murr, L. E. (eds.), Plenum Press, NY and London, p. 299, 1980.

Nadai, A. , *Plasticity*, McGraw-Hill, 1931.

Olson, G. B. , Mescall, J. F. and Azrin, M. , "Adiabatic Deformation and Strain Localization, " Chap. 14, in *Shock Waves and High-Strain-Rate Phenomena in Metals*, Meyers, M. A. , Murr, L. E. (eds.), Plenum Press, NY and London, p. 221, 1980.

Recht, R. F. , "Catastrophic Thermoplastic Shear, " *J. Appl. Mech.* , p. 189, June 1964.

Rice, J. R. , "The Localization of Plastic Deformation, " *Proceedings of the 14th IUTAM Congress*, (Koiter, W. T. , editor), Delft, The Netherlands, North Holland, Amsterdam, 1976.

Rogers, H. C. , "Adiabatic Shearing—A Review, " Drexel Univ. , U. S. Army Research Office, 1974; also see "Adiabatic Plastic Deformation," *Annual Reviews in Materials Science*, Vol. 9, 1979, p. 283.

Rudnicki, J. W. and Rice, J. R. , "Conditions for The Localization of Deformation in Pressure-Sensitive Dilatant Materials, " *J. Mech. Phys. Solids*, Vol. 23, p. 371, 1975.

Staker, M. R. "The Relation between Adiabatic Shear Instability Strain and Materials Properties, " *Acta Metallurgica*, Vol. 29, p. 683, 1981.

Thomas, T. Y. , *Plastic Flow and Fracture in Solids*, Academic Press, 1961.

Truesdell, C. , "General and Exact Theory of Waves in Finite Elastic Strain, " *Arch. Rational Mech. Anal.* , Vol. 8, p. 263, 1961.

Wu, F. H. and Freund, L. B. , "Deformation Trapping Due to Thermoplastic Instability in One Dimensional Wave Propagation, " *J. Mech. Phys. Solids.* , to appear, 1984.

Zee, L. and Sternberg, E. , "Ordinary and Strong Ellipticity in The Equilibrium Theory of Incompressible Hyperelastic Solids, " *Arch. Rat. Mech. and Analysis*, Vol. 83, No. 1, p. 53, 1983.

Zener, C. and Holloman, J. H. , "Effect of Strain Rate Upon Plastic Flow of Steel, " *J. Appl. Phys.* , Vol. 15, p. 22, 1944.

Zienkiewicz, O. C. , *The Finite Element Method*, McGraw-Hill, 3rd ed. , 1977.

APPENDIX

If the strength of the imperfection ϵ is small compared to one, then a regular perturbation analysis may be carried out to obtain linear differential equations for the deviation of the field quantities from their values for the uniform background strain. Due to the presence of the imperfection described in (3.4), the displacement field is assumed to have the form

$$u(t, x_1, x_2) = atx_2 + \epsilon U(t, x_1, x_2) \tag{A.1}$$

The strain components corresponding to (A.1) are

$$u_{,1} = \epsilon U_{,1} \qquad u_{,2} = at + \epsilon U_{,2} \tag{A.2}$$

The expressions (A.1) and (A.2) are substituted into the governing equations (3.2), and all terms are expanded in powers of ϵ. The terms of order zero balance identically. A necessary condition for the terms of order ϵ to balance is

$$U_{,11} + BU_{,22} - AU_{,tt} = -atF_{,2} \tag{A.3}$$

where F is the imperfection shape function as defined in (4.3). The coeficients A and B depend on the ongoing background strain, which implies that A and B are functions of time. For the specific material model being considered here they have the form

$$\begin{aligned} A &= \frac{\rho}{\mu_o\left(1 + \frac{b}{n}a^2t^2\right)^{n-1}} \\ B &= \frac{1 - \frac{b}{n}(1-2n)a^2t^2}{1 + \frac{b}{n}a^2t^2} \end{aligned} \tag{A.4}$$

If $n > 0.5$ then the corresponding homogeneous equation is always hyperbolic because B is always greater than zero no matter how large the uniform background strain. Consequently, all plane waves have real speeds of propagation. However, if $n < 0.5$ then B goes to zero at some time and (A.3) loses

hyperbolicity at this time. The corresponding wave speeds are imaginary. This simple argument suggests the instability of deformation which results from attaining strain levels corresponding to the part of the $\tau - k$ curve with negative slope, and it effectively demonstrates that initially small disturbances will grow large enough to significantly perturb the homogeneous background strain (see also Hayes and Rivlin, 1961) and give rise to the localized shear band.

While it cannot be regarded as a rigorous step in any sense, an estimate of the speed of propagation of the edge of the band may be obtained by examining the equation (A.3) at the instant of time at which $B = 0$. At this instant

$$U_{,11} - AU_{,tt} = -\gamma_o F_{,1} \tag{A.5}$$

where $A = \rho/[\mu_o(1 + \frac{b}{n}a^2t^2)^{n-1}]$. The "wave speed" for propagation in the x_1 direction suggested by this equation is given in (5.1).

FIGURE CAPTIONS

Figure 1: Effective shear stress τ/μ_o vs. effective shear strain k.

Figure 2: The plane of deformation showing a coarse representation of the finite element mesh and the region of the defect.

Figure 3: The nondimensional velocity ϕ for $n = 0.4$ vs. the normalized distance ξ_2 for $\xi_1 = 2d$ and several values of normalized time η.

Figure 4: Shear strain γ_{23} for $n = 0.4$ vs. normalized distance ξ_2 for $\xi_1 = 2d$ and several values of normalized time η.

Figure 5: Nondimensional velocity ϕ for $n = 0.4$ vs. ξ_1 for $\xi_2 = d/4$.

Figure 6: Shear strain γ_{23} for $n = 0.4$ vs. distance ξ_1 at $\xi_2 = d/8$.

Figure 7: The velocity surface ϕ_1 over the ξ_1, ξ_2 plane at time $\eta = 3.6$. The linear velocity distribution in (3.1) has been subtracted out.

Figure 8: The shear strain surface γ_{23} over the ξ_1, ξ_2 plane at time $\eta = 3.6$.

Figure 9: Time history of stress in the stess plane at $\xi_1 = 2d$ and $0 < \xi_2 < d/4$ for $n = 0.4$.

Figure 10: Time history of stress in the stress plane at $\xi_1 = 2d$ and $d/4 < \xi_2 < d/2$ for $n = 0.4$.

Figure 11: Shear strain γ_{23} for $n = 0.5$ vs. distance ξ_2 at $\xi_1 = 2d$ for several values of normalized time η.

Figure 12: Shear strain γ_{23} for $n = 0.5$ vs. distance ξ_1 at $\xi_2 = d/8$ for several values of normalized time η.

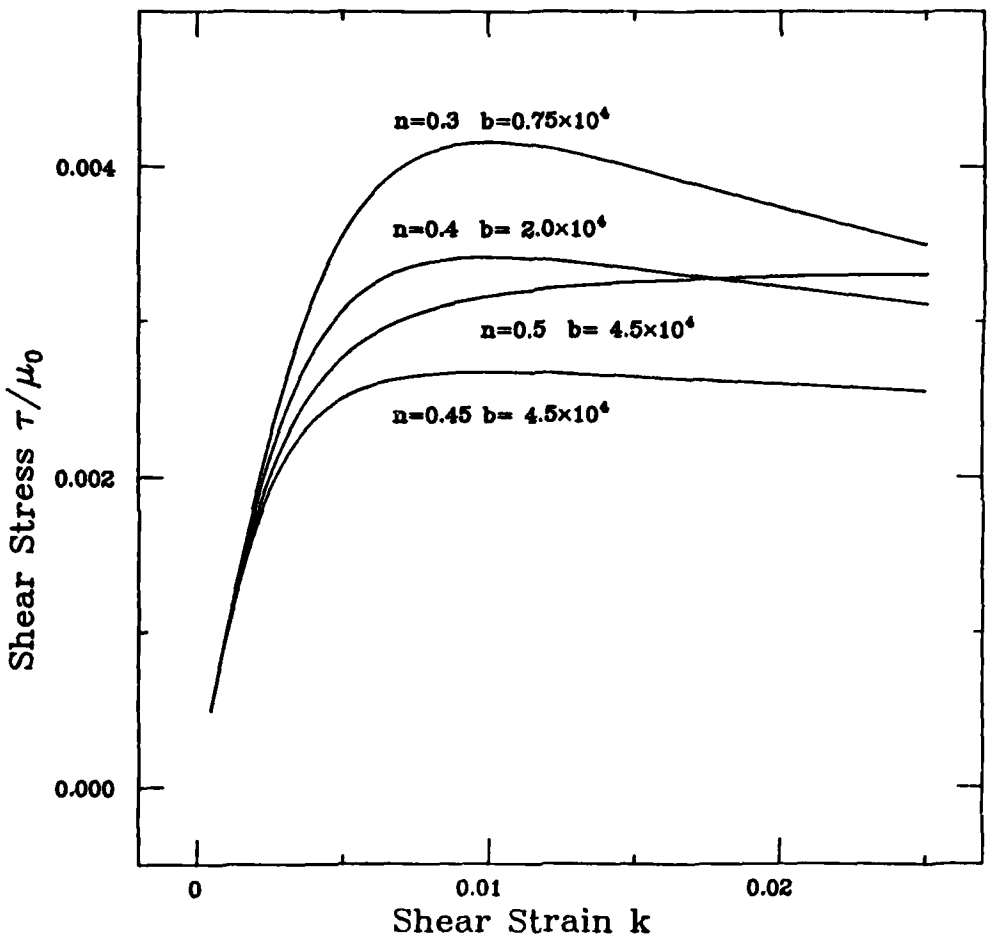
n=0.3 b=0.75×10⁴
n=0.4 b= 2.0×10⁴
n=0.5 b= 4.5×10⁴
n=0.45 b= 4.5×10⁴
0.004
0.002
0.000
Shear Stress τ/μ_0
0
0.01
0.02
Shear Strain k

Figure 1

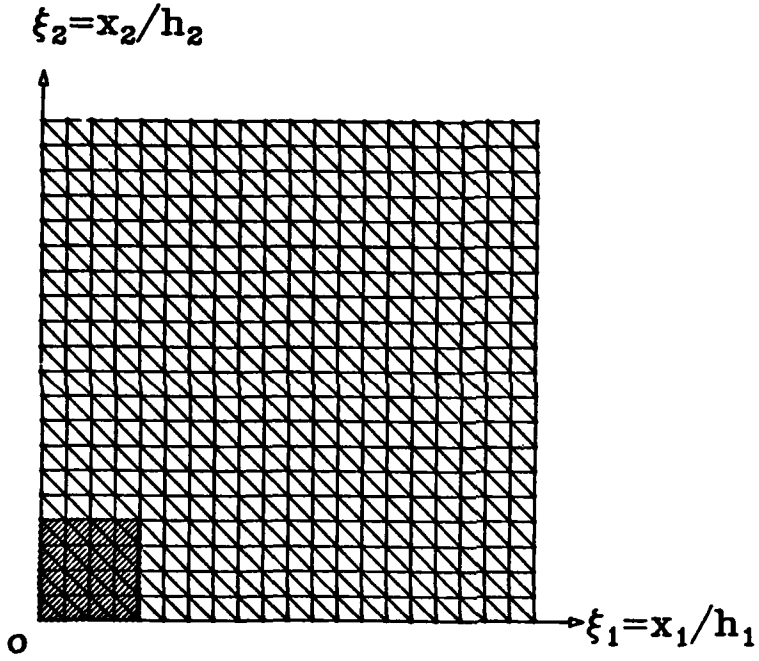

Figure 2

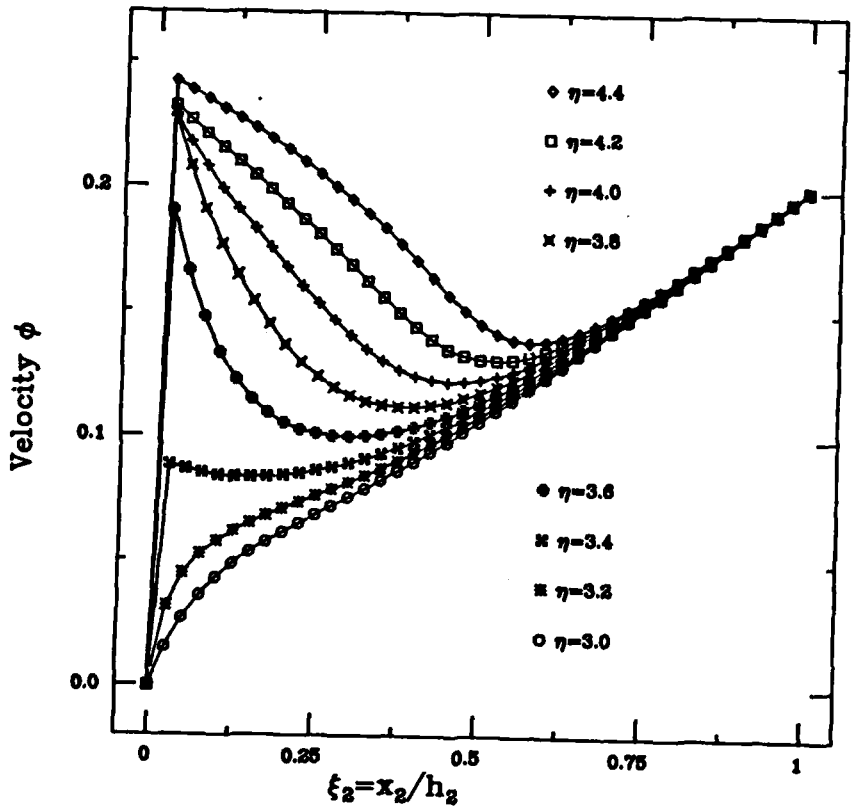
η=4.4
η=4.2
η=4.0
η=3.8
η=3.6
η=3.4
η=3.2
η=3.0
Velocity φ
0.0
0.1
0.2
0
0.25
0.5
0.75
1
ξ2=x2/h2

Figure 3

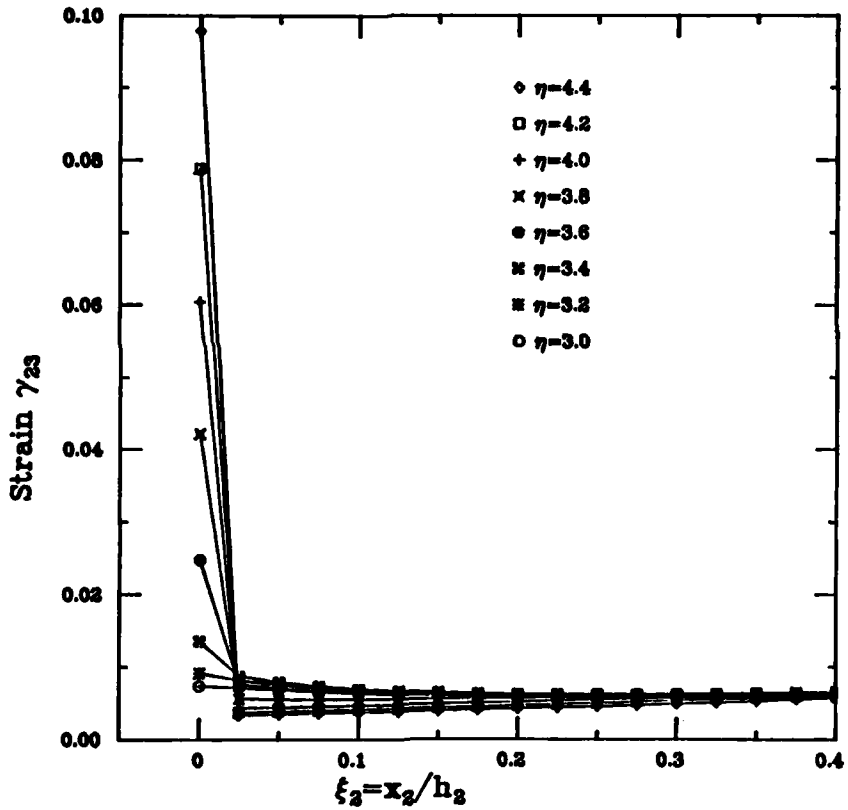
0.10
0.08
0.06
0.04
0.02
0.00
0
0.1
0.2
0.3
0.4
Strain γ_{23}
$\xi_2=x_2/h_2$
η=4.4
η=4.2
η=4.0
η=3.8
η=3.6
η=3.4
η=3.2
η=3.0

Figure 4

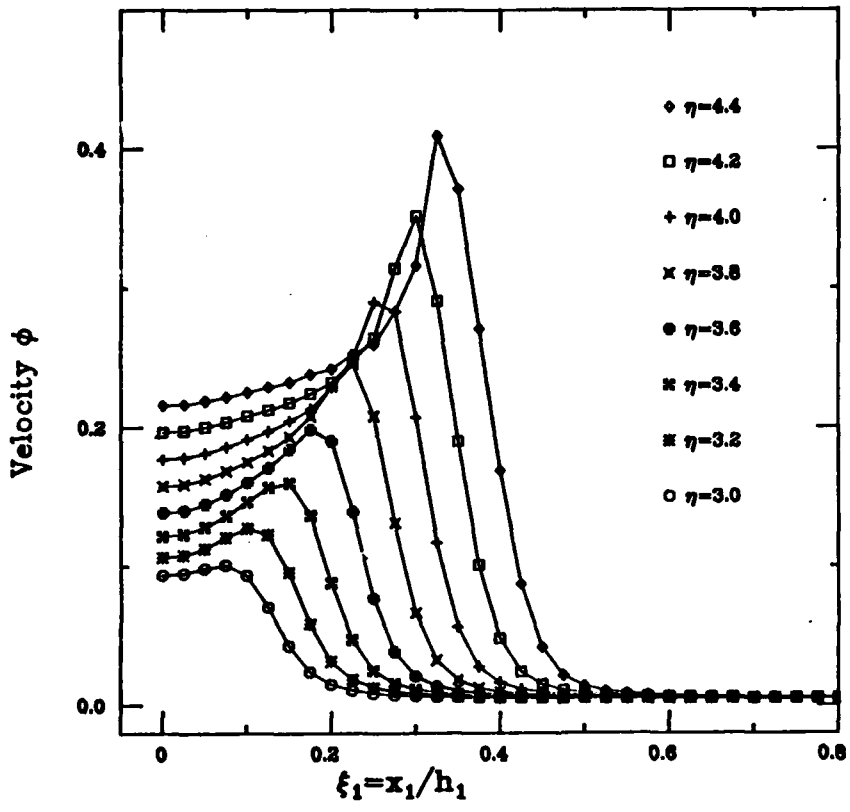
Velocity ϕ
0.0
0.2
0.4
0
0.2
0.4
0.6
0.8
$\xi_1=x_1/h_1$
η=4.4
η=4.2
η=4.0
η=3.8
η=3.6
η=3.4
η=3.2
η=3.0

Figure 5

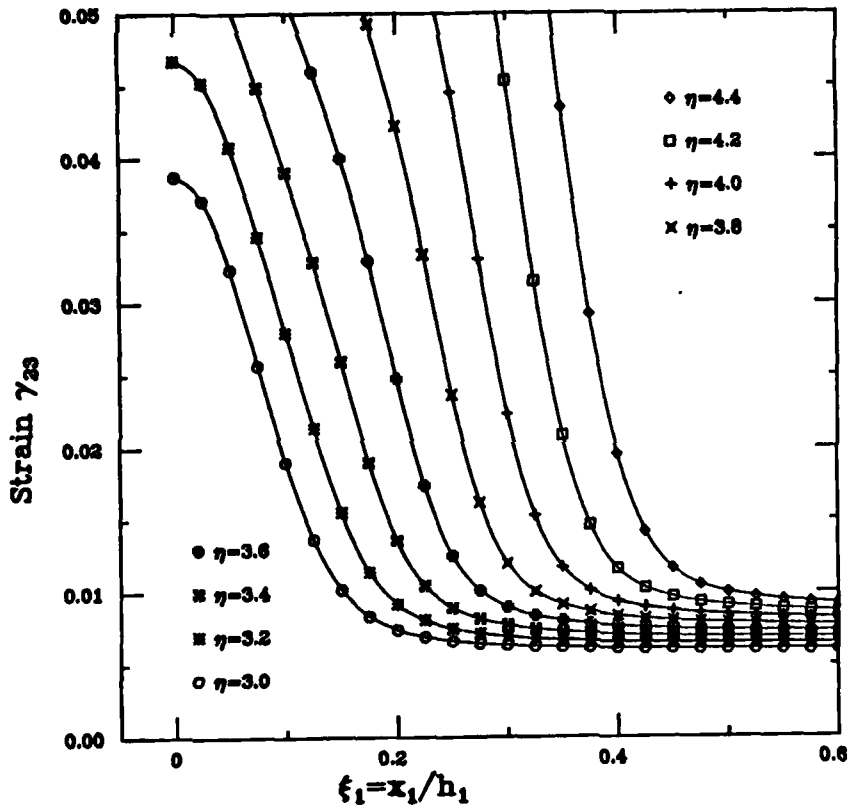
0.05
0.04
0.03
0.02
0.01
0.00
0
0.2
0.4
0.6
Strain γ_{23}
$\xi_1=x_1/h_1$
◇ η=4.4
□ η=4.2
+ η=4.0
× η=3.8
● η=3.6
■ η=3.4
■ η=3.2
○ η=3.0

Figure 6

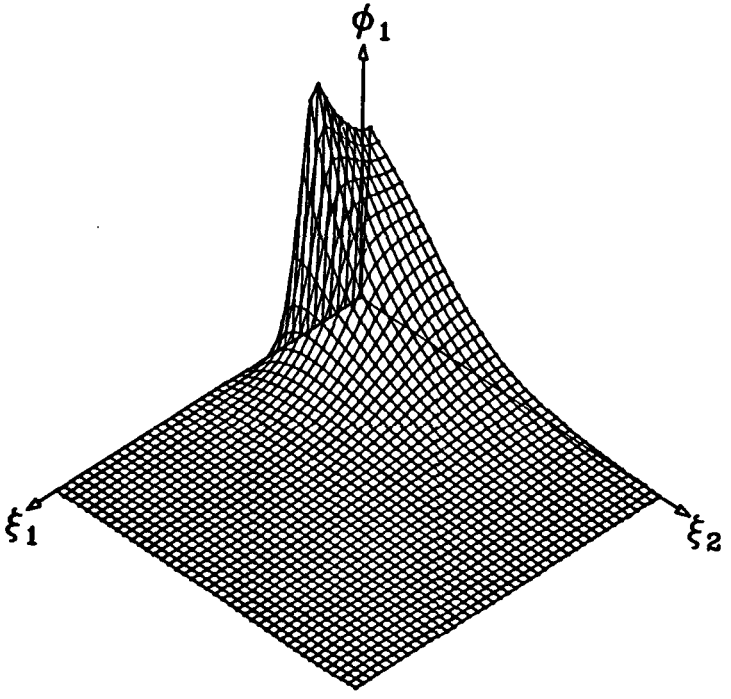

Figure 7

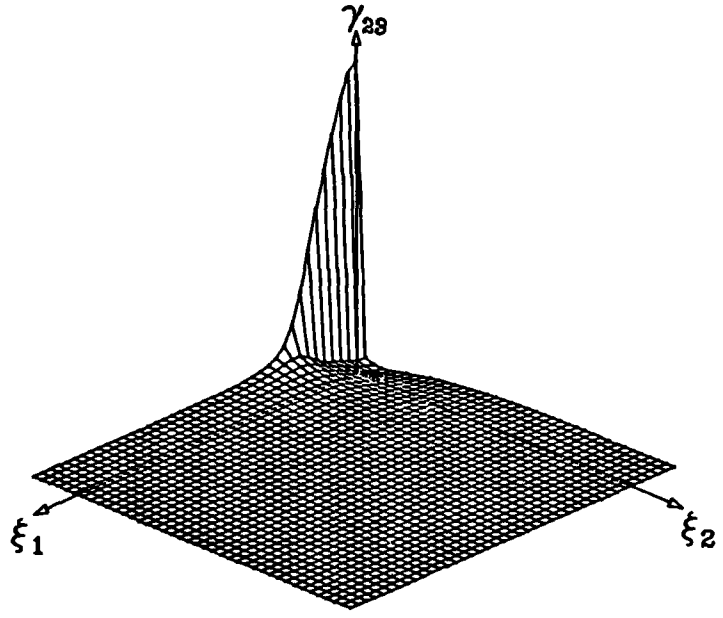

Figure 8

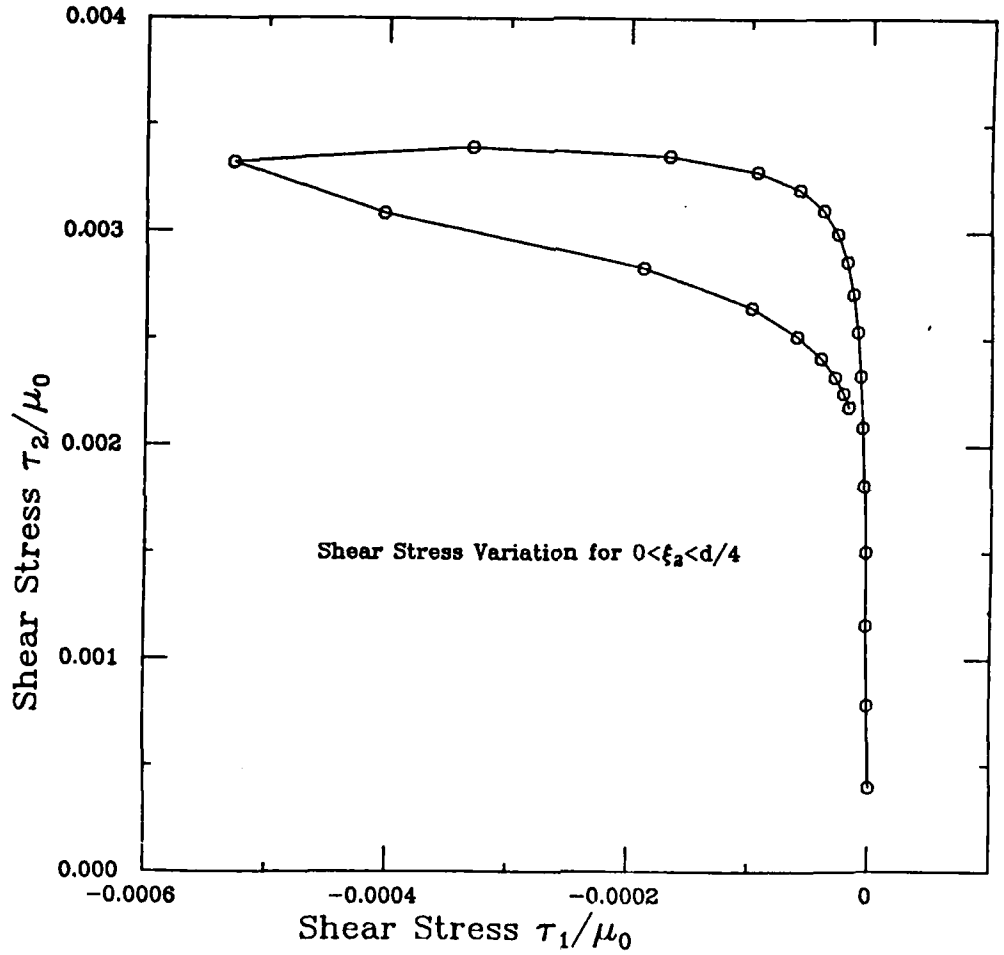
0.004
0.003
0.002
0.001
0.000
Shear Stress τ_2/μ_0
Shear Stress Variation for $0<\xi_a<d/4$
−0.0006
−0.0004
−0.0002
0
Shear Stress τ_1/μ_0

Figure 9

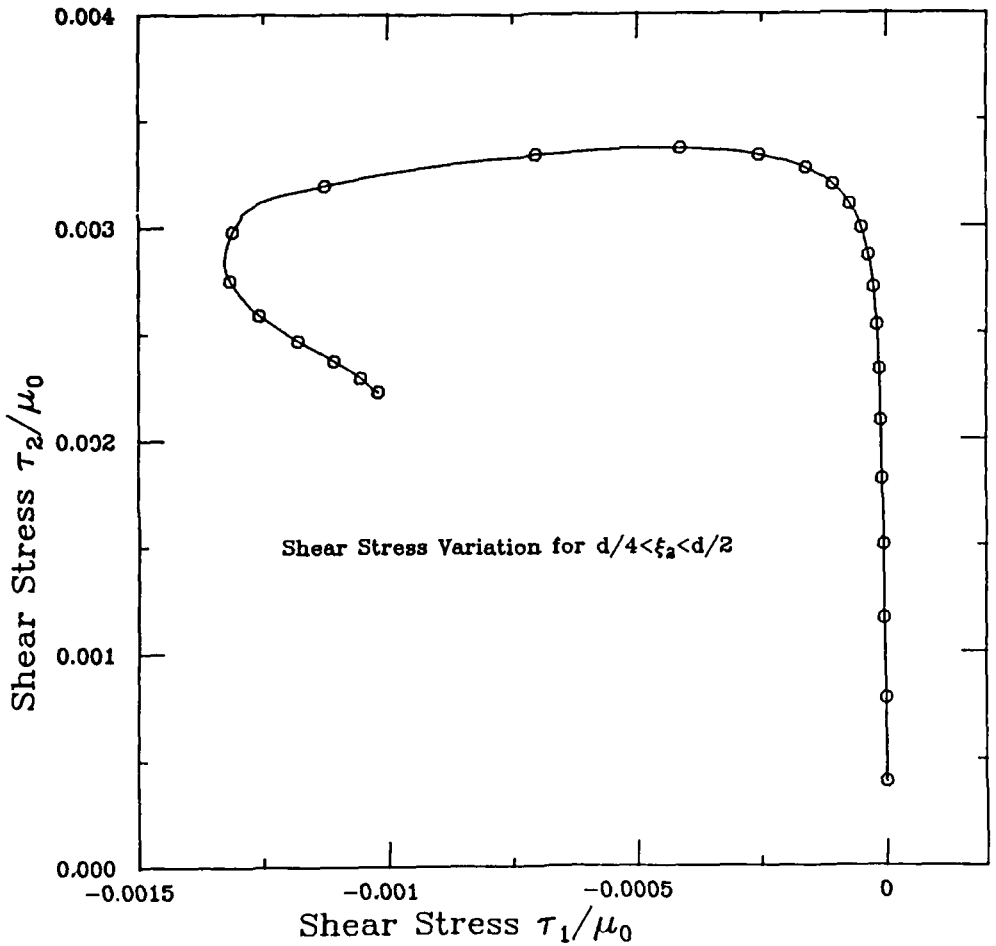
0.004
0.003
0.002
0.001
0.000
Shear Stress τ_2/μ_0
Shear Stress Variation for $d/4<\xi_a<d/2$
−0.0015
−0.001
−0.0005
0
Shear Stress τ_1/μ_0

Figure 10

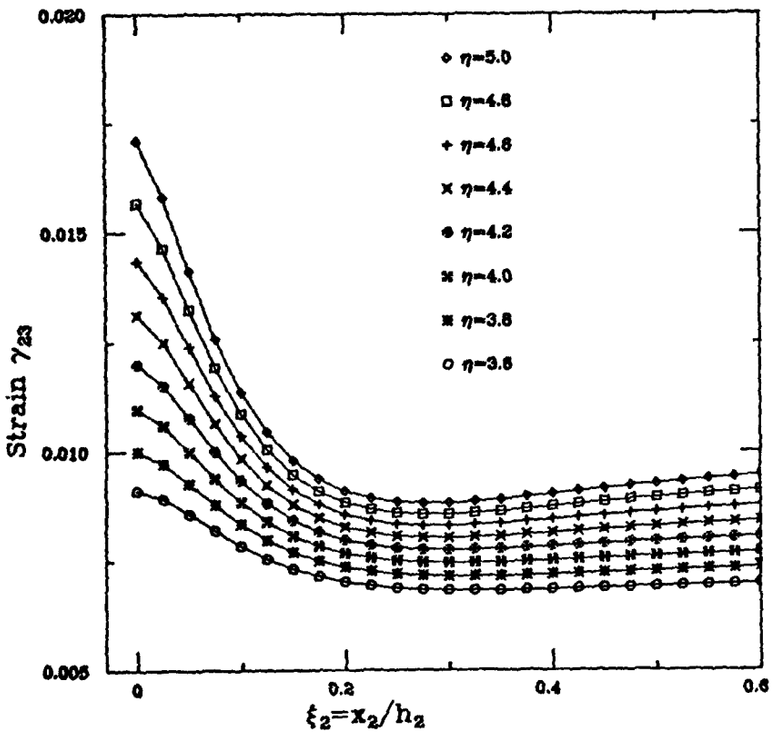
0.020
0.015
0.010
0.005
Strain γ_{23}
0
0.2
0.4
0.6
$\xi_2=x_2/h_2$
η=5.0
η=4.8
η=4.6
η=4.4
η=4.2
η=4.0
η=3.8
η=3.6

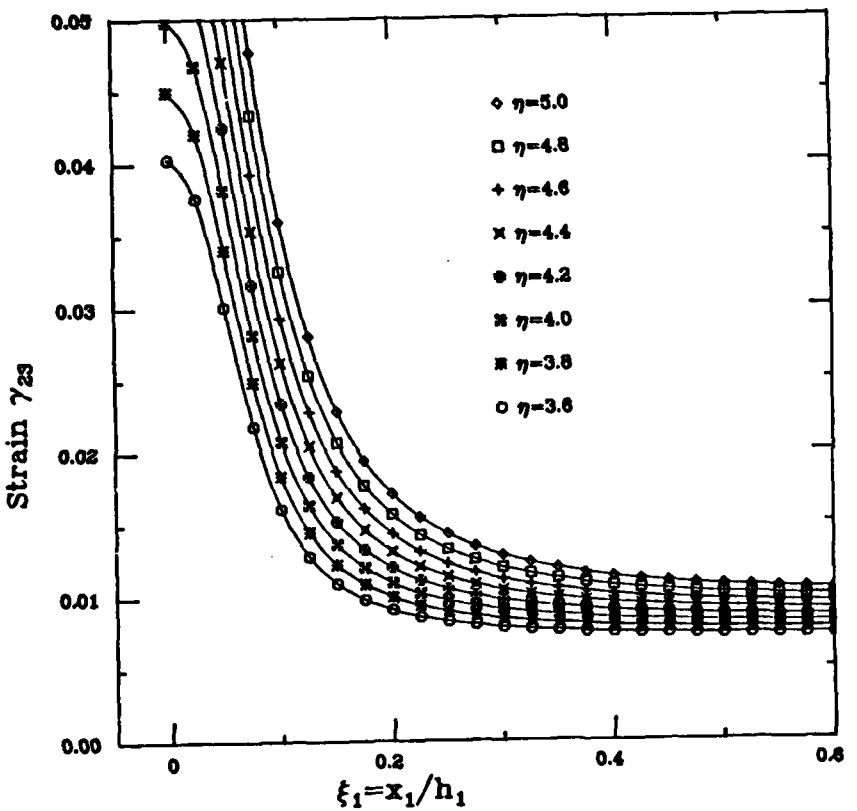
0.05
0.04
0.03
0.02
0.01
0.00
Strain γ_{23}
0
0.2
0.4
0.6
$\xi_1=x_1/h_1$
η=5.0
η=4.8
η=4.6
η=4.4
η=4.2
η=4.0
η=3.8
η=3.6

Figure 12